



Published in final edited form as:

*Gastroenterology*. 2016 December ; 151(6): 1232–1244.e10. doi:10.1053/j.gastro.2016.07.045.

## Loss of Trefoil Factor 2 From Pancreatic Duct Glands Promotes Formation of Intraductal Papillary Mucinous Neoplasms in Mice

Junpei Yamaguchi<sup>1</sup>, Mari Mino-Kenudson<sup>2</sup>, Andrew S. Liss<sup>1</sup>, Sanjib Chowdhury<sup>3</sup>, Timothy C. Wang<sup>4</sup>, Carlos Fernández-del Castillo<sup>1</sup>, Keith D. Lillemoe<sup>1</sup>, Andrew L. Warshaw<sup>1</sup>, and Sarah P. Thayer<sup>1,3</sup>

<sup>1</sup>Andrew L. Warshaw Institute for Pancreatic Cancer Research, Department of Surgery, Massachusetts General Hospital, Boston, MA

<sup>2</sup>Department of Pathology, Massachusetts General Hospital, Boston, MA

<sup>3</sup>Division of Surgical Oncology and the Fred & Pamela Buffett Cancer Center, University of Nebraska Medical Center, Omaha, NE

<sup>4</sup>Division of Digestive & Liver Diseases and Irving Cancer Research Center, Columbia University Medical Center, New York, NY

### Abstract

**Background & Aims**—Little is known about the origin of pancreatic intraductal papillary mucinous neoplasms (IPMN). Pancreatic duct glands (PDGs) are gland-like outpouches budding off the main pancreatic ducts that function as progenitor niche for the ductal epithelium; they express gastric mucins and have characteristics of side-branch IPMN. We investigated whether PDGs are a precursor compartment for IPMN and the role of trefoil factor family 2 (TFF2)—a protein expressed by PDGs and the gastric mucosa that are involved in epithelial repair and tumor suppression.

**Methods**—We obtained pancreatectomy specimens from 20 patients with chronic pancreatitis, 13 with low-grade side-branch IPMN, and 15 patients with PDAC; histologically normal pancreata were used as controls (n=18). Samples were analyzed by immunohistochemistry to detect TFF1 and TFF2 and cell proliferation. We performed mitochondrial DNA mutational mapping studies to determine the cell lineage and fate of PDG cells. *Pdx1-Cre;LSL-KRAS<sup>G12D</sup>* (KC) mice were bred with TFF2-knockout mice to generate *KC/Tff2<sup>-/-</sup>* and *+/-* mice. Pancreata were collected and histologically analyzed for formation of IPMN, pancreatic intraepithelial neoplasias, and PDAC, in

---

**Corresponding author:** Sarah P. Thayer, MD, PhD, sarah.thayer@unmc.edu, University of Nebraska Medical Center, 986345 Nebraska Medical Center, Omaha, NE 68198-6345, Phone: (402)-559-7298, Fax: (402)-559-7900.

**Publisher's Disclaimer:** This is a PDF file of an unedited manuscript that has been accepted for publication. As a service to our customers we are providing this early version of the manuscript. The manuscript will undergo copyediting, typesetting, and review of the resulting proof before it is published in its final citable form. Please note that during the production process errors may be discovered which could affect the content, and all legal disclaimers that apply to the journal pertain.

**Disclosures:** All authors are free of conflicts of interest and have nothing to disclose.

**Contributors:** JPY, ASL, SC, SPT: Conception and design, collection and assembly of data, interpretation of data, manuscript writing. SPT, CFC, ALW: Administrative support. MMK: Data analysis and interpretation of pathology. KL, TCW: Review of manuscript. SPT: Final approval of manuscript.

addition to proliferation and protein expression. Human pancreatic ductal epithelial cells and PDAC cell lines were transfected with vectors to overexpress or knock down TFF2 or SMAD4.

**Results**—Histologic analysis of human samples revealed gastric-type IPMN to comprise 2 molecularly distinct layers: a basal crypt segment that expressed TFF2 and overlying papillary projections. Proliferation occurred predominantly in the PDG-containing basal segments. Mitochondrial mutation mapping revealed a 97% match between the profiles of proliferating PDG cells and their overlying non-proliferative IPMN cells. In contrast to KC mice, 2-month-old *KC/Tff2+/-* and *KC/Tff2-/-* mice developed prominent papillary structures in the duct epithelium with cystic metaplasia of the PDG, which resembled human IPMN; these expressed gastric mucins (MUC5AC and MUC6) but not the intestinal mucin MUC2. *KC/TFF2*-knockout mice developed a greater number and higher grade of pancreatic intraepithelial neoplasias than KC mice, and 1 mouse developed an invasive adenocarcinoma. Expression of TFF2 reduced proliferation of PDAC cells 3-fold; this effect required upregulation and activation of SMAD4. We found expression of *TFF2* to be downregulated in human PDAC by hypermethylation of its promoter.

**Conclusions**—In histologic analyses of human IPMNs, we found PDGs to form the basal segment and possibly serve as a progenitor compartment. TFF2 has tumor suppressor activity in the mouse pancreas and prevents formation of mucinous neoplasms.

### Keywords

Pancreatic tumorigenesis; carcinogenesis; gene regulation; PanIN

## INTRODUCTION

Intraductal papillary mucinous neoplasms (IPMN) are commonly identified cystic pancreatic neoplasms that are precursor lesions of pancreatic ductal adenocarcinoma (PDAC)<sup>1–5</sup>. Histologically, these cystic lesions are characterized by mucin-producing epithelia with a distinct papillary structure. Morphologically, they are classified into two broad groups: Main-duct and side-branch IPMN<sup>4</sup>. While main-duct IPMN (MD-IPMN) are characterized by a markedly dilated main pancreatic duct filled with thick mucin and are mostly associated with an intestinal epithelial subtype, side-branch IPMN (SB-IPMN) are characterized by a cyst or cluster of cysts budding off the main duct, and are most often associated with a gastric epithelial subtype. Recent reports suggest that approximately 3% of all abdominal cross-sectional imaging studies show asymptomatic pancreatic branch cysts<sup>6</sup>. Only a small percentage of these SB-IPMN will progress to invasive cancer. However, when cancer does arise, it is histologically and biologically indistinguishable from PDAC<sup>7</sup>. Thus, SB-IPMN pose a major health issue, which underscores the importance of understanding how these originate and what contributes to their progression to cancer.

There have been a number of reports describing peribiliary glands (PBG) with biliary tree stem/progenitors at the bottom of the glands<sup>8,9</sup>. PBG are characterized as tubulo-alveolar glands with mucinous and serous glandular acini located in the deeper tissue of the bile duct walls<sup>10</sup>. In the pancreatic duct system, similar to the PBG, our group recently identified and characterized pancreatic duct glands (PDG). The PDG are normal gland-like outpouches budding off pancreatic ducts which function as progenitor niche for ductal epithelium and

expresses gastric mucins (MUC6) and trefoil factor family 2 (TFF2)<sup>11, 12</sup>. They exhibit a gastric phenotype distinct from the overlying pancreatic duct epithelia. In response to inflammation, PDG exhibit increased proliferative activity, supplying new cells to the overlying main duct epithelium<sup>12</sup>. In response to injury, PDG can also undergo a mucinous metaplasia, upregulate expression of mucin 6 (MUC6) and TFF2, and exhibit *de novo* expression of MUC5AC. The size, number, and complexity of PDG after the inflammatory injury are reminiscent of SB-IPMN. Furthermore, IPMN have been reported to have high expression of TFF2 rather than normal ductal epithelium<sup>13</sup>, suggesting a possible link between PDG and IPMN.

The architecture and the molecular signature of the PDG most resemble those of gastric pyloric glands. Of particular interest, was the expression of TFF2 within the PDG compartment. TFF2 is one of three members of the trefoil factor family of protease resistant proteins found throughout the gastrointestinal (GI) system. The trefoil factor family has been well known to play an important role in epithelial repair by promoting cell migration (restitution) and is up-regulated in response to injury<sup>14-17</sup>. In the stomach, TFF2 also plays an important role in the anti-inflammatory defense mechanism and functions as a tumor suppressor. Mice deficient in TFF2 have been found to have accelerated gastric neoplasia in both *H. pylori*-infected mice and the genetic gp130(F/F) mouse model<sup>18, 19</sup>. Clinically, TFF2 is often silenced by promoter hypermethylation in gastric cancer<sup>20</sup>. These reports suggest that TFF2 functions not only as the promoter of mucosal restitution, but also as a tumor suppressor to prevent the progression of cancer.

In this study, we evaluated the characteristics of PDG and performed mitochondrial mutational fate mapping in human samples to investigate the lineage relationship between PDG and IPMN. Immunohistochemistry (IHC) and mitochondrial mapping suggest that PDG are the compartment of origin for IPMN tumor cells. Furthermore, in mice we find that the combination of TFF2-deficiency in the setting of mutant KRAS *in vivo* results in the development of IPMN lesions. *In vitro*, over-expression of TFF2 inhibits the proliferation of pancreatic cancer cells via a SMAD4-mediated mechanism. Furthermore, the TFF2 promoter is transcriptionally silenced by DNA hypermethylation in PDAC. These results suggest that IPMN may arise from PDG due to deficiency or dysfunction of TFF2, which possesses some qualities of a tumor suppressor.

## MATERIAL AND METHODS

### Human Samples

Human samples were collected and analyzed in accordance with an Institutional Review Board-approved protocol. Histologically normal control pancreata (n=18) were obtained from organ donors. Samples of chronic pancreatitis (n=20), low-grade SB-IPMN (n=13) and PDAC (n=15) were obtained from pancreatectomy specimens.

### Mouse Samples

**Chronic Pancreatitis Model**—All experiments were approved by the Massachusetts General Hospital Subcommittee on Research Animal Care. Chronic pancreatitis was induced

in healthy C57BL/6 mice (Jackson Lab; n=21) of either sex by 3 series of cerulein injections per week for periods of 2 weeks. Each series of injections comprised 8 hourly intraperitoneal injections of 50 µg/kg cerulein (Sigma, St Louis, MO).

**Genetically Engineered Mouse Models**—The Pdx1-Cre; LSL-KRAS<sup>G12D</sup> mice were generously provided by Nabeel Bardeesy (Massachusetts General Hospital)<sup>21, 22</sup>. These strains were bred with TFF2-KO mice, kindly provided by Timothy Wang (Columbia University)<sup>23</sup> to generate the genotypes, Pdx1-Cre; LSL-KRAS<sup>G12D</sup>; TFF2-KO (KC/TFF2-KO). BrdU was injected into the peritoneum 2 hours before harvesting the pancreata.

### Histology and Immunohistochemistry

IHC was performed using antibodies shown in Supplemental Table 1. The sections were incubated overnight at 4°C with each primary antibody and incubated for 1 h at room temperature with biotinylated secondary antibodies diluted to 1:1000 or fluorescently labelled secondary antibodies diluted to 1:500. The specimens were developed using DAB-Plus Substrate Kit (Invitrogen) and counterstained with hematoxylin, while samples processed for immunofluorescence were stained with 4',6-diamidino-2-phenylindole (DAPI).

### Laser Capture Micro-dissection and Mitochondrial DNA Sequencing

FFPE specimens of IPMN slides (n=4) were subjected to laser capture micro-dissection. After evaluation for Ki-67 positivity, cells were captured using Arcturus PixCell Iie (Arcturus, CA, USA). In each patient, 3–4 lesions were selected. Ten to 30 cells were captured and their DNA extracted using QIAamp DNA FFPE Tissue Kit (Qiagen). The extracted DNA was amplified using a Single Cell Whole Genome Amplification Kit (WGA4; Sigma). DNA was further amplified by PCR reaction using 6 overlapping primer pairs for the D-loop of the mitochondrial genome (Supplemental Table 2). PCR products were cleaned by ExoSAP-IT (Affymetrix), followed by bidirectional Sanger sequencing on an ABI 3730XL DNA Analyzer.

### Cell Culture Study

Human pancreatic ductal epithelial (HPDE) cells<sup>24, 25</sup> were cultured in keratinocyte-SFM (Invitrogen) and human PDAC cell lines were maintained in DMEM. 10mM BrdU was added in the medium for BrdU assay. Control vector (pCMV-SPORT6), TFF2-overexpression plasmid (Thermo Fisher Scientific), control shRNA vector (pGFP-V-RS), and SMAD4-shRNA (OriGene) were transfected into PDAC cell lines using Effectene (Qiagen) according to the manufacturer's protocol. SMARTpool ON-TARGETplus TFF2 siRNA and ON-TARGETplus Non-Targeting Control Pool (Scramble siRNA) were transfected into PDAC cell lines (PANC-1 and Aspc-1) using DharmaFECT 1 transfection reagent according to manufacturer's protocol (Dharmacon GE Healthcare). Recombinant Human TFF2 protein from R&D Systems (catalogue # 8290-TF) and transfected in PANC-1 and Aspc-1 cells as per published report<sup>26</sup>.

## Western Blotting

Proteins were extracted from cultured pancreatic cancer cells. 25 µg of the protein was subjected to 10% SDS-polyacrylamide electrophoresis and transferred to a nitrocellulose membrane, which was incubated with primary antibodies against TFF2 (rabbit polyclonal, Protein Tech, 1:500) and SMAD4 (rabbit monoclonal, clone EP618Y, abcam, 1:1000) then detected using a chemiluminescence kit (Supersignal West Pico, Thermo Scientific), or visualized using an Odyssey IR Scanner (LI-COR Biosciences) system and LI-COR secondary fluorescent antibodies.

## RT-PCR and qPCR

Total RNA (1 µg) was extracted from cultured cells using an RNA extraction kit (RNeasy Mini; Qiagen) and used to synthesize cDNA (ThermoScript PT-PCR System; Invitrogen). PCR amplification was performed in a total volume of 50 µl containing 2 µl of cDNA, 2mM MgCl<sub>2</sub>, 200 mM dNTP Mix, 0.2 mM each of 5'- and 3'-primers, and 1U of Platinum Taq DNA polymerase (Invitrogen). The two-step quantitative real time PCR (qPCR) using TaqMan reagents was performed according to manufacturer's protocol (Applied Biosystems).

## Methylation Pyrosequencing

Bisulfite treatment was carried out using 1000 ng of sample genomic DNA and the EZ DNA Methylation-Direct kit (Zymo Research, Orange, CA). PCR reactions were performed with 42 ng of bisulfite-modified DNA in a total volume of 25 µl for 35 cycles using primer pairs shown in Supplemental Table 3. Methylation percentage of each CpG was determined using a Qiagen (Valencia, CA) Pyromark Q96 pyrosequencer, according to manufacturers' recommendations.

## Statistics

All statistical analysis was performed using SPSS-II and GraphPad Prism 6 software. Differences between the two groups were analyzed using ANOVA. When the P-value was 0.01, the difference was regarded as significant.

## RESULTS

### IPMN and PDG Share Similarities in Location, Mucin Expression, and Molecular Signature

Human SB-IPMN have many characteristics similar to those of inflamed PDG, both are morphologically cystic lesions budding off the main pancreatic duct (Figure 1A). We now demonstrate that PDG can also undergo a cystic hypertrophy that results in the formation of small mucinous cysts along the main pancreatic duct, which are similar in morphology to SB-IPMN. Histologically, the epithelia of both chronically inflamed PDG and SB-IPMN are noted to be tall, columnar and mucin-containing with basally located nuclei (Figure 1B). The epithelia of both are characterized as a gastric foveolar type. In the inflamed PDG and IPMN, IHC demonstrated the up-regulated expression of deep and superficial gastric mucins, MUC6 and MUC5AC, as well as gastric mucin-related molecules TFF1 and TFF2 (Figure 1C). Among these mucin-related molecules, TFF2 is uniquely and specifically

expressed in PDG as shown in our previous work<sup>12</sup>. Neither the associated ductal epithelium, nor any other compartments of the pancreas expresses TFF2, suggesting that TFF2 is a unique marker for PDG.

### **PDG Comprise the Basal Segment of the Large Papillary Projections of IPMN**

IHC of human samples revealed that TFF2 was highly expressed in the bottom layer/crypt, but infrequently identified in overlying papillary projections of IPMN, suggesting that the bottom layer of IPMN consist of PDG (Figure 2A, B). PDGs can also be recognized by histologic evaluation of human SB-IPMN specimens, which demonstrates expansion and crowding of hyperplastic PDG against the overlying epithelium (Figure 2A, H&E left). However, in IPMN with typical papillary structure, the PDG compartment is not histologically evident (Figure 2A, H&E right). To better define the contribution and location of the PDG epithelium within IPMN, we employed IHC using MUC6, MUC5AC, TFF1, and TFF2. IHC of SB-IPMN (Figure 2A) revealed that MUC6-positive (green) and TFF2-positive (yellow) PDG are not only closely associated with the base of the IPMN (Figure 2A, asterisk), but also found at the crypt-like basal layer of IPMN (Figure 2A, arrow). IHC evaluation of IPMN with papillary structure revealed TFF2-positive PDG cells in the bottom layer/crypts between each papillary structure (Figure 2A, right). Quantification of TFF2 expression in IPMN and PDAC specimens revealed that TFF2 is highly expressed (92.3%, 12/13) in the bottom-PDG layer, but infrequently identified in overlying papillary projections of IPMN (7.7%, 1/13) and PDAC (Figure 2B). Thus, PDG are not only closely associated with the overlying cyst wall, but compose the basal segment of large papillary projections.

### **PDG are the Site of Epithelial Proliferation within IPMN**

The complex relationship between the PDG and the overlying IPMN have been divided into three histologic types: Hyperplastic PDG, cystic metaplasia and papillary structure (Figure 2C). The cystic metaplasia is characterized by cystic expansion of the hyperplastic PDG compartments, which are frequently found to open into the lumen of the IPMN, creating a crypt or pseudopapillary structure. In the papillary structure, PDG are found to form the basal segments opening up directly to the cystic lumen. Of the 13 samples evaluated, hyperplasia was found in 7/13, cystic metaplasia in 9/13, and papillary in 13/13 samples. These three types are closely associated and frequently overlap possibly representing progressive histologic changes.

In order to determine whether PDG are the proliferative compartment of human SB-IPMN, we performed IHC for Ki-67 (Figure 2C, bottom). Ki-67-positive cells are found predominantly in the PDG compartment. To better characterize the relationship between PDG and the proliferative compartment, single and double IHC for Ki-67 and TFF2 were performed (Figures 3A and 3B), revealing that each PDG and the adjoining walls of the overlying papillary projections form a functional unit that we have termed a PDG-IPMN unit (Figure 3C). Ki-67-positive cells are found in each PDG-IPMN unit, located between the TFF2-positive PDG cells and the overlying IPMN, suggesting that the upper border of the PDG is the site of IPMN cell genesis. Interestingly, PanIN found in large pancreatic ducts also shows a similar association with hyperplastic PDG, which similarly has TFF2 and

Ki-67 expression (Supplemental Figure 1), suggesting that PDG are likely the source of early mucinous neoplasms, such as IPMN and PanIN.

### **The Non-proliferative IPMN Segments have a Similar Mutational Profile to their Proliferating Parent PDG within the PDG-IPMN Unit**

To investigate the lineage relationship between proliferating cells of the PDG and overlying IPMN epithelium, we used mitochondrial DNA (mtDNA) mutational analysis of IPMN/PDG units in human samples. Because of the relatively high mutation rate of mtDNA, mutational mapping of its sequence has been a powerful tool for tracking evolutionary relationship, relatedness of populations, and tracing cell lineage<sup>27–29</sup>. If the cells of the papillary structures originate from the proliferating cells of the PDG, then each pair within the IPMN/PDG unit should have a similar mutation profile. Multiple PDG/IPMN units from 4 different patients were evaluated. Within each unit, 10 to 30 Ki-67-positive PDG cells and the overlying IPMN epithelia were isolated by laser capture microscopy (LCM) (Figure 3D). Normal pancreatic duct epithelium was used as a matched reference. The mtDNA sequencing of the D-loop revealed 85 different mutations (Figure 3E, Supplemental Table 4). The mutational profiles of the Ki-67-positive PDG progenitor cells matched those of the overlying non-proliferating IPMN cells 96.4% of the time (188/195 matched pairs). A permutation test (randomization test) was used to assess the association across the entire ensemble of mtDNA genetic markers. This revealed that the mtDNA mutational matches between the PDG and overlying IPMN are statistically significant, with  $p=0.0012$ . These data support a genetic lineage relationship between PDG and the overlying IPMN, suggesting that the cells of PDG and IPMN are from the same origin. Given that PDG are the proliferating compartments of IPMN and have been previously characterized as a progenitor compartment needed for normal pancreatic epithelial renewal<sup>12</sup>, it is likely that IPMN tumor cells are descendants of the PDG.

### **Loss of TFF2 in Mice results in PDG Hyperplasia and the Formation of IPMN-like Lesions**

TFF2 is uniquely expressed in PDG and has been shown to possess tumor suppressor-like qualities in gastric cancer<sup>30</sup>. To explore the hypothesis that TFF2 functions as a tumor suppressor in PDG, we employed a genetically engineered mouse model of pancreatic cancer with TFF2 deficiency (KC/TFF2<sup>-/-</sup>). The characteristics of PDG and ductal epithelium were evaluated first at 2- and 4-month time points in KC mice (n=6 at 2 months old and n=6 at 4 months old), KC/TFF2<sup>+/-</sup> mice (n=10 at 2 months old and n=9 at 4 months old), and KC/TFF2<sup>-/-</sup> mice (n=9 at 2 months old and n=8 at 4 months old). In the KC/TFF2<sup>-/-</sup> group at the age of 2 months, a significant increase in the size and number of PDG was observed, and the lining cells of PDG showed micro-papillary changes (Figure 4A, Supplemental Figure 2). Additionally, an almost 6-fold increase in proliferative activity in the PDG compartment was observed in both the KC/TFF2<sup>+/-</sup> and the KC/TFF2<sup>-/-</sup> (Figure 4B). Interestingly, there was no difference in proliferative activity between KC/TFF2<sup>+/-</sup> and KC/TFF2<sup>-/-</sup> mice, indicating that heterozygous loss of TFF2 was sufficient to induce proliferation in PDG.

In control KC mice, there were no metaplastic changes at the age of 2 months. Micro-papillary lesions were found only in a limited area of the main pancreatic duct in 4-month-

old mice. In contrast to KC-control mice, 2-month-old KC/TFF2<sup>+/-</sup> and KC/TFF2<sup>-/-</sup> mice developed prominent papillary structures in the duct epithelium with cystic metaplasia of the PDG, which had a striking resemblance to human IPMN (Figure 4A). These lesions were found predominantly in the main pancreatic duct, but the small branch ducts also showed similar changes. By 4 months, severe atypical cells were found in some KC/TFF2<sup>-/-</sup> mice (Figure 4C, Supplemental Table 5). The molecular characteristics of these papillary structures were investigated by IHC (Figure 4D), which demonstrated that they expressed gastric mucins, such as MUC5AC and MUC6, but not the intestinal mucin MUC2, indicating that they were more similar to gastric-type IPMN rather than the intestinal type.

### Loss of TFF2 Accelerates mPanIN Formation in KRAS Mice

Loss of TFF2 also results in accelerated PanIN formation at slightly later time points. Mice were harvested at the age of 6 months (KC mice: n=7, KC/TFF2<sup>+/-</sup>: n=6 and KC/TFF2<sup>-/-</sup> mice: n=6). In control KC mice, scattered mPanIN-1 lesions that were distributed widely across mouse pancreata were found, while mPanIN-2 and -3 lesions were rarely observed, consistent with previous reports<sup>31</sup>. In contrast, KC/TFF2<sup>-/-</sup> and KC/TFF2<sup>+/-</sup> mice showed a dramatic increase of mPanIN development (Figure 5A, top). The majority of these lesions were still only early mPanIN-1; however, a few more mPanIN-2 and mPanIN-3 lesions were observed in KC/TFF2<sup>+/-</sup> and KC/TFF2<sup>-/-</sup> mice (Figure 5A, bottom). The PanIN-occupying area was calculated and compared, revealing a 4–6 fold increase in the KC/TFF2KO group (Figure 5B). In one of 6 mice, an invasive adenocarcinoma developed in the pancreatic head with multiple metastases present in both liver and lung (Figure 5C). These results suggest that the loss of TFF2 not only plays a role in IPMN formation, but may also be important in PanIN-PDAC carcinogenesis.

### TFF2 Suppress Proliferation of Pancreatic Cancer Cells *in vitro*

To further explore the role of TFF2 as a tumor suppressor for the pancreas, immortalized HPDE cells and pancreatic cancer cell lines (Aspc-1, BxPc3, Colo357, KP-1NL, and PANC-1) were studied *in vitro*. HPDE and 4 of the 5 pancreatic cancer cell lines examined lacked or showed very low levels of TFF2 expression (Figure 6A, Supplemental Figure 3). To investigate the effect of TFF2 expression on proliferation, a TFF2-overexpression construct was transfected into PANC-1 cells. Proliferative activity was further evaluated by a BrdU incorporation assay and showed that TFF2 suppresses proliferation greater than 3-fold in the PANC-1 cancer cell line (Supplemental Figure 4). Growth curves reveal a dose-dependent effect (Figure 6B).

### Tumor-suppressive Role of TFF2 Depends on SMAD4 *in vitro*

Recent reports suggest that loss of SMAD4 combined with KRAS activation may result in IPMN formation<sup>21, 22</sup>. To determine whether the tumor-suppressive role of TFF2 might be mediated, in part, through SMAD4, we evaluated SMAD4 expression after ectopic expression of TFF2 in PANC-1 cells. There was an increase of SMAD4 expression identified 2 days after TFF2 overexpression (Figure 6C). Other cell lines with an intact SMAD4 gene (MiaPACA-2 and Colo357)<sup>32–35</sup> showed a similar upregulation of SMAD4 in response to TFF2 overexpression (Supplemental Figure 5A). Additionally, treatment of PANC-1 and Aspc-1 cells with recombinant human TFF2 peptide for 24 hours resulted in



SMAD4 up regulation (Supplemental Figures 6A and 6B). Immunofluorescence revealed that SMAD4, initially localized in the cytoplasm, was found in both the nuclear and cytoplasmic compartments after ectopic expression of TFF2 (Figure 6D). Taken together, these results demonstrate that TFF2 can regulate SMAD4.

To investigate whether the anti-proliferative activity of TFF2 is dependent on SMAD4, a TFF2-overexpressing vector and shRNA against SMAD4 were co-transfected into PANC-1 cells. Enhanced TFF2 and suppressed SMAD4 expression were confirmed at protein level (Supplemental Figure 5B). An immunofluorescent study revealed that PANC-1 cells with TFF2 expression does not incorporate BrdU; however, when SMAD4 expression was suppressed in TFF2-positive cells, proliferation appeared to be effectively restored (Figure 6E). This was also confirmed by quantitation of the percentage of BrdU positive cells (Figure 6F). To further assess the requirement of SMAD4 in the anti-proliferative effects of TFF2, SMAD4-null (BxPC3 and Cfpac-1) and SMAD4-mutated (Capan-1) PDAC cell lines were tested<sup>32</sup>. TFF2 overexpression in these cell lines did not show the anti-proliferative effects of TFF2 (Supplemental Figure 7). These results, in aggregate, suggest that SMAD4 is a downstream effector of TFF2, and that its upregulation and activation are required for TFF2 anti-proliferative effects on cancer cells.

### **TFF2 Promoter Methylation and SMAD4 Regulation in vitro**

To investigate possible epigenetic regulation of TFF2 in pancreatic cancer cells, native TFF2 promoter methylation was analyzed by pyrosequencing. PANC-1 and AsPC-1 cells showing low and high expression of TFF2, respectively (Figure 6A), were selected for this study. A total of 5 CpG sites within the TFF2 promoter, from -181 to -149 from the transcriptional start site were examined by pyrosequencing<sup>19</sup>. In PANC-1 cells with low expression of TFF2, the 5 CpG sites were hypermethylated. In contrast, TFF2 expressing AsPC-1 cells showed CpG hypomethylation (Figure 7A). Pyrosequencing of native TFF2 promoter methylation was also performed on the HPDE cells. TFF2 is not expressed in HPDE cells consistent which is consistent with the identification that the 5 CpG sites on TFF2 promoter were hypermethylated (Supplemental Figure 8A). However, TFF2 overexpression for 48 hours in HPDE cells resulted in an upregulation of SMAD4 mRNA similar to pancreatic cancer cell lines (Supplemental Figure 8B).

PANC-1 and AsPC-1 cells were treated with decitabine<sup>36</sup>, a hypomethylating agent, and then analyzed for their expression of TFF2 by qPCR. Decitabine treatment for 72 hours resulted in a dose-dependent increase in TFF2 mRNA in both PANC-1 and AsPC-1 cell lines (Figure 7B), which accompanied the demethylation of the CpG sites (Figure 7C). The mean change in percentage of CpG methylation was >60% for both cell lines.

To determine if TFF2 upregulation by decitabine can upregulate SMAD4, PANC-1 cells were treated for 4 days with decitabine and analyzed for the expression of SMAD4 by qPCR. We found that SMAD4 was upregulated by nearly 4 fold. However, when TFF2 levels were reduced by siRNA knockdown, decitabine-mediated upregulation of SMAD4 was abrogated (Figure 7D). These data support the hypothesis that methylation of the TFF2 promoter may be an early mechanism in the inactivation of the tumor suppressor-like qualities of TFF2 in PDAC.

## DISCUSSION

Our study reveals that the PDG compartments form the basal part of the papillary structure of IPMN and are the principal site of proliferation. IPMN are composed of multiple PDG/IPMN units giving rise to their characteristic papillary projections. Mitochondrial DNA mutational mapping revealed that the proliferative zone of the PDG/IPMN unit has the same mutational profile as the overlying IPMN cells, suggesting that IPMN tumor cells may be descendants of PDG cells. Furthermore, loss of TFF2 from the PDG compartment resulted in development of IPMN and PanIN lesions, suggesting that TFF2 has some tumor suppressor activity and that this effect is mediated in part by SMAD4.

Identifying a role for PDG in early inflammation-mediated metaplasia would be an important step toward elucidating the early events of the IPMN and PanIN carcinogenesis. Our previously published work revealed that PDG are an epithelial progenitor compartment important for epithelial renewal in response to acute inflammatory injury<sup>12</sup>, and in response to chronic injury, this compartment undergoes a Shh-dependent gastrointestinal metaplasia, taking on many features that resemble pancreatic cancer precursor lesions, PanIN and IPMN<sup>11</sup>. We show in this work that loss of TFF2 *in vivo* results in acceleration of tumorigenesis of the pancreas, which suggests that the PDG may be the compartment of origin for both IPMN and PanIN. Interestingly risk factors for PDAC, such as Type-2 diabetes and chronic pancreatitis, have been shown to specifically stimulate the PDG glands in mice and pancreatitis can upregulate TFF2 expression in PDG<sup>12</sup>. Although much work needs to be done to understand the mechanism underpinning of cancer, it appears that autoinduction of TFF2 after inflammatory injury plays a role to inhibit neoplasia, and that the dysregulation of key regenerative pathways unique to the PDG, such as overexpression of Shh and loss of TFF2, can lead to metaplasia and ultimately neoplasia.

The morphologic mechanisms for a PDG to architecturally become a mature IPMN remains to be determined; however, in evaluating the complex structures of PDG and IPMN there appear to be three distinct histologic types that were closely associated with one another, which could possibly represent progressive histologic changes from hyperplastic PDG to cystic metaplasia, ultimately forming mature papillary structures. Molecularly, one of the key regulators of the conversion from PDG to tumor cells is likely to be the down regulation of TFF2.

The role of TFF2 as tumor suppressor was initially uncovered in the field of gastric tumorigenesis<sup>18–20, 37</sup>. Loss of TFF2 in a genetically engineered mouse model of gastric cancer (gp130 mouse) results in an increased proliferation and larger tumors. In addition, TFF2<sup>-/-</sup> mice with chronic infection of *H. pylori* develop more advanced gastric dysplasia, including carcinoma *in situ*<sup>17, 18</sup>. It is still unclear the mechanism that TFF2 exerts its tumor suppressive activity. Although this work reveals it has anti-proliferative properties, it has also been shown to possess anti-inflammatory properties and modify the body's immune response<sup>37</sup>. TFF2 can negative regulate myeloid progenitor cells, a cell type found to promote GI carcinogenesis<sup>38</sup>. In pancreatic carcinogenesis, the loss of TFF2 is not an initiating genetic event, but it appears to accelerate KRAS-dependent neoplasia, consistent with its possible role as a tumor-suppressor gene. Interestingly, heterozygous loss of TFF2

was able to promote the development of IPMN and PanIN lesions, suggesting that haplosufficiency of TFF2 may be promote tumorigenesis.

Loss or downregulation of TFF2 in PDAC likely uses an epigenetic mechanism, a mechanism seen in gastric carcinogenesis<sup>18</sup>. There have been no reported cases of TFF2 mutations. Furthermore, mutational analysis in 91 human PDAC samples failed to identify insertion, deletion, nonsense, or frameshift mutations (data not shown). Recent studies suggest that treatment of mouse models of PDAC with decitabine slows cancer progression and extends survival<sup>36</sup>, which could be due, in part, to upregulation of TFF2.

Our data also suggest an interaction of two tumor suppressor genes, SMAD4 and TFF2. Genetically engineered KC mice combined with loss of SMAD4 similarly resulted in the formation of both IPMN and PanIN<sup>20</sup>. Thus, it is noteworthy that our *in vitro* studies showed TFF2 exerts its anti-proliferative effects, in part, via SMAD4. Much work still remains to be done to elucidate the mechanisms and roles TFF2 and SMAD4 in human IPMN/PanIN pathogenesis.

Although much remains to be done to understand how dysregulation of the PDG, a pancreatic ductal epithelial progenitor compartment, contributes to the formation of pancreatic IPMN and PanIN, this work reveals that PDG may be the compartment of origin for both and that TFF2 has tumor suppressor activity, which may, in part, be regulated by SMAD4. Thus PDG may be the link between IPMN and PanIN however the downstream programs that orchestrates the development of these distinct tumors remains to be understood.

## Supplementary Material

Refer to Web version on PubMed Central for supplementary material.

## Acknowledgments

**Grant Support:** This work was supported in part by 7P01CA117969-07 (SPT) and the Warshaw Institute for Pancreatic Cancer Research (SPT, ASL, JY).

## Abbreviations

|             |  |
|-------------|--|
| <b>IHC</b>  | Immunohistochemistry                     |
| <b>IPMN</b> | Intraductal papillary mucinous neoplasms |
| <b>PDG</b>  | Pancreatic duct glands                   |
| <b>TFF</b>  | Trefoil factor family                    |

## REFERENCES

Author names in bold designate shared co-first authors.

1. Tanaka M, Fernandez-del Castillo C, Adsay V, et al. International consensus guidelines 2012 for the management of IPMN and MCN of the pancreas. *Pancreatology*. 2012; 12:183–197. [PubMed: 22687371]
2. Hruban RH, Adsay NV, Albores-Saavedra J, et al. Pancreatic intraepithelial neoplasia: a new nomenclature and classification system for pancreatic duct lesions. *Am J Surg Pathol*. 2001; 25:579–586. [PubMed: 11342768]
3. Furukawa T, Kloppel G, Volkan Adsay N, et al. Classification of types of intraductal papillary-mucinous neoplasm of the pancreas: a consensus study. *Virchows Arch*. 2005; 447:794–799. [PubMed: 16088402]
4. Ban S, Naitoh Y, Mino-Kenudson M, et al. Intraductal papillary mucinous neoplasm (IPMN) of the pancreas: its histopathologic difference between 2 major types. *Am J Surg Pathol*. 2006; 30:1561–1569. [PubMed: 17122512]
5. Katabi N, Klimstra DS. Intraductal papillary mucinous neoplasms of the pancreas: clinical and pathological features and diagnostic approach. *J Clin Pathol*. 2008; 61:1303–1313. [PubMed: 18703569]
6. Laffan TA, Horton KM, Klein AP, et al. Prevalence of unsuspected pancreatic cysts on MDCT. *AJR Am J Roentgenol*. 2008; 191:802–807. [PubMed: 18716113]
7. Mino-Kenudson M, Fernandez-del Castillo C, Baba Y, et al. Prognosis of invasive intraductal papillary mucinous neoplasm depends on histological and precursor epithelial subtypes. *Gut*. 2011; 60:1712–1720. [PubMed: 21508421]
8. Wang Y, Lanzoni G, Carpino G, et al. Biliary tree stem cells, precursors to pancreatic committed progenitors: evidence for possible life-long pancreatic organogenesis. *Stem Cells*. 2013; 31:1966–1979. [PubMed: 23847135]
9. Carpino G, Cardinale V, Onori P, et al. Biliary tree stem/progenitor cells in glands of extrahepatic and intrahepatic bile ducts: an anatomical in situ study yielding evidence of maturational lineages. *J Anat*. 2012; 220:186–199. [PubMed: 22136171]
10. Nakanuma Y, Hosono M, Sanzen T, et al. Microstructure and development of the normal and pathologic biliary tract in humans, including blood supply. *Microsc Res Tech*. 1997; 38:552–570. [PubMed: 9330346]
11. Strobel O, Rosow DE, Rakhlin EY, et al. Pancreatic duct glands are distinct ductal compartments that react to chronic injury and mediate Shh-induced metaplasia. *Gastroenterology*. 2010; 138:1166–1177. [PubMed: 20026066]
12. Yamaguchi J, Liss AS, Sontheimer A, et al. Pancreatic duct glands (PDGs) are a progenitor compartment responsible for pancreatic ductal epithelial repair. *Stem Cell Res*. 2015; 15:190–202. [PubMed: 26100232]
13. Terris B, Blaveri E, Crnogorac-Jurcevic T, et al. Characterization of gene expression profiles in intraductal papillary-mucinous tumors of the pancreas. *Am J Pathol*. 2002; 160:1745–1754. [PubMed: 12000726]
14. Taupin D, Podolsky DK. Trefoil factors: initiators of mucosal healing. *Nat Rev Mol Cell Biol*. 2003; 4:721–732. [PubMed: 14506475]
15. Hoffmann W. Trefoil factors TFF (trefoil factor family) peptide-triggered signals promoting mucosal restitution. *Cell Mol Life Sci*. 2005; 62:2932–2938. [PubMed: 16374581]
16. Wright NA, Poulosom R, Stamp G, et al. Trefoil peptide gene expression in gastrointestinal epithelial cells in inflammatory bowel disease. *Scand J Gastroenterol Suppl*. 1992; 193:76–82. [PubMed: 1290063]
17. Alison MR, Chinery R, Poulosom R, et al. Experimental ulceration leads to sequential expression of spasmodic polypeptide, intestinal trefoil factor, epidermal growth factor and transforming growth factor alpha mRNAs in rat stomach. *J Pathol*. 1995; 175:405–414. [PubMed: 7790995]
18. Fox JG, Rogers AB, Whary MT, et al. Accelerated progression of gastritis to dysplasia in the pyloric antrum of TFF2 –/– C57BL6 x Sv129 *Helicobacter pylori*-infected mice. *Am J Pathol*. 2007; 171:1520–1528. [PubMed: 17982128]
19. Peterson AJ, Menheniott TR, O'Connor L, et al. *Helicobacter pylori* infection promotes methylation and silencing of trefoil factor 2, leading to gastric tumor development in mice and humans. *Gastroenterology*. 2010; 139:2005–2017. [PubMed: 20801119]

20. Leung WK, Yu J, Chan FK, et al. Expression of trefoil peptides (TFF1, TFF2, and TFF3) in gastric carcinomas, intestinal metaplasia, and non-neoplastic gastric tissues. *J Pathol.* 2002; 197:582–588. [PubMed: 12210076]
21. Bardeesy N, Aguirre AJ, Chu GC, et al. Both p16(Ink4a) and the p19(Arf)-p53 pathway constrain progression of pancreatic adenocarcinoma in the mouse. *Proc Natl Acad Sci U S A.* 2006; 103:5947–5952. [PubMed: 16585505]
22. Bardeesy N, Cheng KH, Berger JH, et al. Smad4 is dispensable for normal pancreas development yet critical in progression and tumor biology of pancreas cancer. *Genes Dev.* 2006; 20:3130–3146. [PubMed: 17114584]
23. Farrell JJ, Taupin D, Koh TJ, et al. TFF2/SP-deficient mice show decreased gastric proliferation, increased acid secretion, and increased susceptibility to NSAID injury. *J Clin Invest.* 2002; 109:193–204. [PubMed: 11805131]
24. Ouyang H, Mou L, Luk C, et al. Immortal human pancreatic duct epithelial cell lines with near normal genotype and phenotype. *Am J Pathol.* 2000; 157:1623–1631. [PubMed: 11073822]
25. Furukawa T, Duguid WP, Rosenberg L, et al. Long-term culture and immortalization of epithelial cells from normal adult human pancreatic ducts transfected by the E6E7 gene of human papilloma virus 16. *Am J Pathol.* 1996; 148:1763–1770. [PubMed: 8669463]
26. Dubeykovskaya Z, Dubeykovskiy A, Solal-Cohen J, et al. Secreted trefoil factor 2 activates the CXCR4 receptor in epithelial and lymphocytic cancer cell lines. *J Biol Chem.* 2009; 284:3650–3662. [PubMed: 19064997]
27. Taylor RW, Turnbull DM. Mitochondrial DNA mutations in human disease. *Nat Rev Genet.* 2005; 6:389–402. [PubMed: 15861210]
28. McDonald SA, Greaves LC, Gutierrez-Gonzalez L, et al. Mechanisms of field cancerization in the human stomach: the expansion and spread of mutated gastric stem cells. *Gastroenterology.* 2008; 134:500–510. [PubMed: 18242216]
29. Greaves LC, Preston SL, Tadrous PJ, et al. Mitochondrial DNA mutations are established in human colonic stem cells, and mutated clones expand by crypt fission. *Proc Natl Acad Sci U S A.* 2006; 103:714–719. [PubMed: 16407113]
30. Kurt-Jones EA, Cao L, Sandor F, et al. Trefoil family factor 2 is expressed in murine gastric and immune cells and controls both gastrointestinal inflammation and systemic immune responses. *Infect Immun.* 2007; 75:471–480. [PubMed: 17101660]
31. Hingorani SR, Petricoin EF, Maitra A, et al. Preinvasive and invasive ductal pancreatic cancer and its early detection in the mouse. *Cancer Cell.* 2003; 4:437–450. [PubMed: 14706336]
32. Deer EL, González-Hernández J, Coursen JD, et al. Phenotype and genotype of pancreatic cancer cell lines. *Pancreas.* 2010; 39:425–435. [PubMed: 20418756]
33. Chen WB, Lenschow W, Tiede K, et al. Smad4/DPC4-dependent regulation of biglycan gene expression by transforming growth factor-beta in pancreatic tumor cells. *J Biol Chem.* 2002; 277:36118–36128. [PubMed: 12140283]
34. Sun C, Yamato T, Furukawa T, et al. Characterization of the mutations of the K-ras, p53, p16, and SMAD4 genes in 15 human pancreatic cancer cell lines. *Oncol Rep.* 2001; 8:89–92. [PubMed: 11115575]
35. Moore PS, Sipos B, Orlandini S, et al. Genetic profile of 22 pancreatic carcinoma cell lines: Analysis of K-ras, p53, p16 and DPC4/Smad4. *Virchows Arch.* 2001; 439:798–802. [PubMed: 11787853]
36. Shakya R, Gonda T, Quante M, et al. Hypomethylating therapy in an aggressive stroma-rich model of pancreatic carcinoma. *Cancer Res.* 2013; 73:885–896. [PubMed: 23204224]
37. Baus-Loncar M, Kayadimir T, Takaishi S, et al. Trefoil factor family 2 deficiency and immune response. *Cell Mol Life Sci.* 2005; 62:2947–2955. [PubMed: 16374583]
38. Asfaha S, Dubeykovskiy AN, Tomita H, et al. Mice that express human interleukin-8 have increased mobilization of immature myeloid cells, which exacerbates inflammation and accelerates colon carcinogenesis. *Gastroenterology.* 2013; 144:155–166. [PubMed: 23041326]

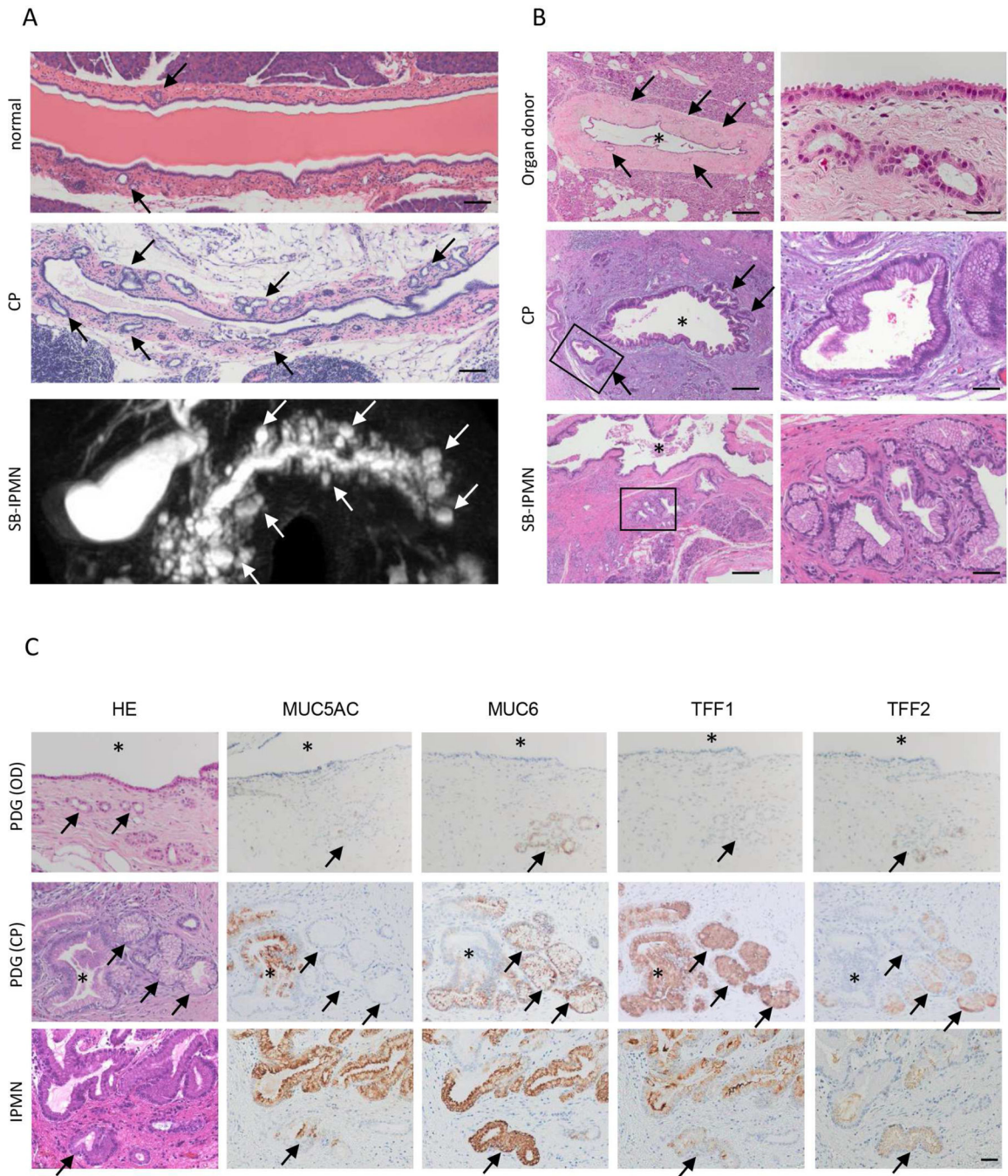


**Figure 1.** PDG are reminiscent of SB-IPMN in humans. (A) In response to inflammatory injury, PDG (top and middle, arrow) increase in size and number. These structural characteristics of inflamed PDG are reminiscent of human SB-IPMN (bottom, arrow). Scale Bar: 200  $\mu$ m (B) The lining cells of PDG (top) become mucinous and columnar in response to inflammatory injury (middle). This mucinous appearance is reminiscent of SB-IPMN (bottom). Asterisks show the lumen of the main duct. Scale Bars: 200  $\mu$ m (left), 20  $\mu$ m (right, OD) and 50  $\mu$ m (right, CP and IPMN). (C) Both inflamed PDG and SB-IPMN show upregulated expressions

of gastric mucins (MUC5AC and MUC6) and TFFs. Arrow: PDG, asterisk: pancreatic duct.  
Scale Bars: 50  $\mu$ m.

Author Manuscript

Author Manuscript

Author Manuscript

Author Manuscript

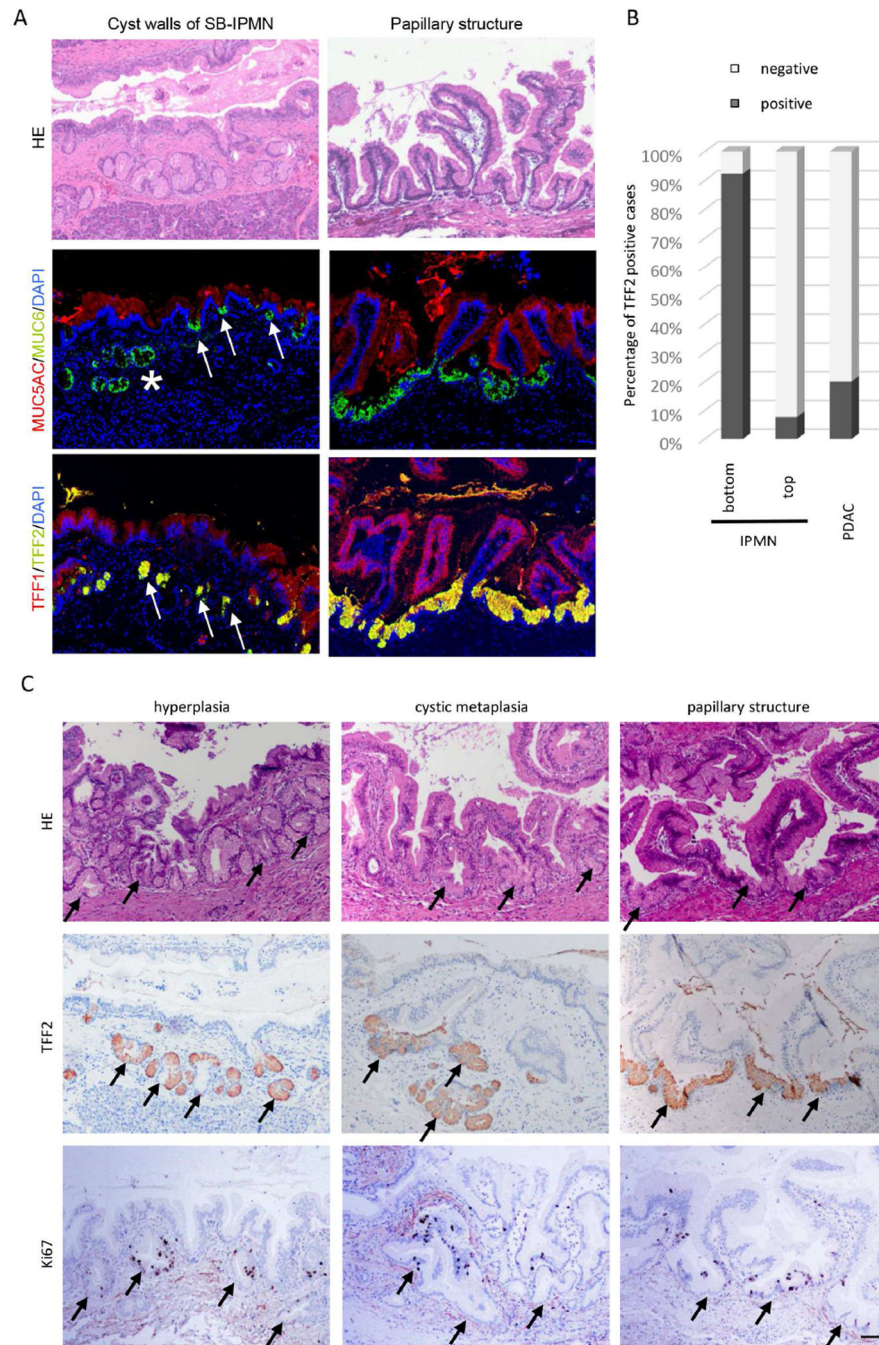


**Figure 2.** PDG comprise the basal segment of SB-IPMN in humans. (A) The cyst walls of SB-IPMN demonstrate expansion and crowding of hyperplastic PDG (left) PDG are identified by MUC6 (green) and TFF2 (yellow). They are seen to fuse (asterisk) and open into the IPMN cyst wall (arrow). PDG are also found in the bottom layer/crypts between each papillary structure of IPMN (right). Scale Bars: 100  $\mu$ m. (B) Quantification of TFF2 expression in IPMN (n=13) and PDAC (n=15). (C) Three different histologic patterns of PDG (arrow) within SB-IPMN. The hyperplastic phase (left), the cystic metaplasia phase (middle) and the



papillary phase (right). Each PDG can be identified by its expression of TFF2, and Ki-67-positive proliferating cells are found in the PDG compartment (bottom). Scale Bars: 100  $\mu$ m.

Author Manuscript

Author Manuscript

Author Manuscript

Author Manuscript

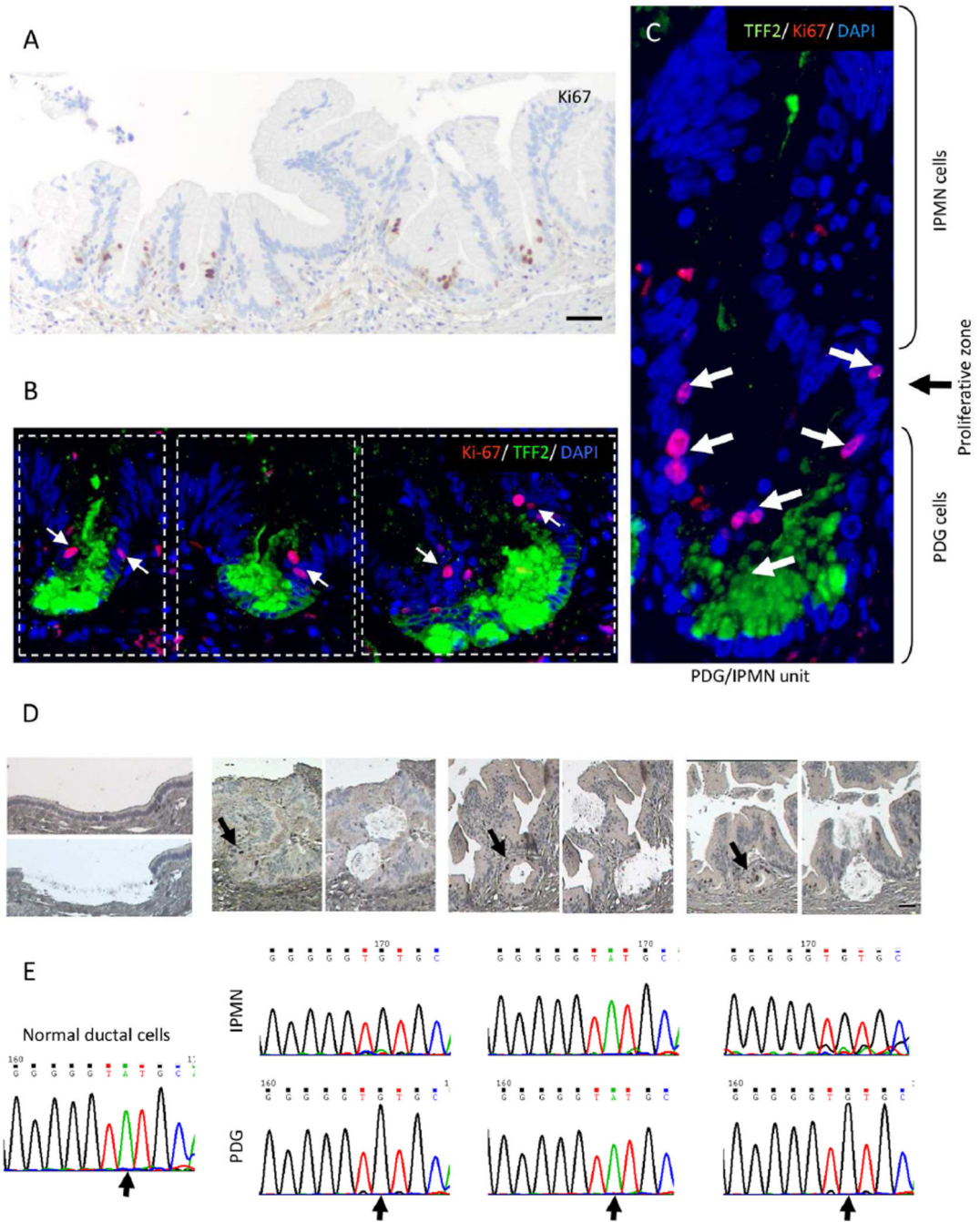


**Figure 3.** Human IPMN are comprised of multiple PDG/IPMN units. The dotted frame outlines three PDG/IPMN units. (A, B, C) Proliferation (Ki-67; arrow) occurs in a narrow zone located between the TFF2-positive PDG and the overlying IPMN. Scale Bars: 50  $\mu$ m (D) Within each PDG/IPMN unit, Ki-67-positive PDG cells and their overlying IPMN epithelia were isolated by LCM. Scale Bars: 50  $\mu$ m (E) The D-loops of mitochondrial DNA reveal the same mutational profile (arrow) in each PDG/IPMN unit.

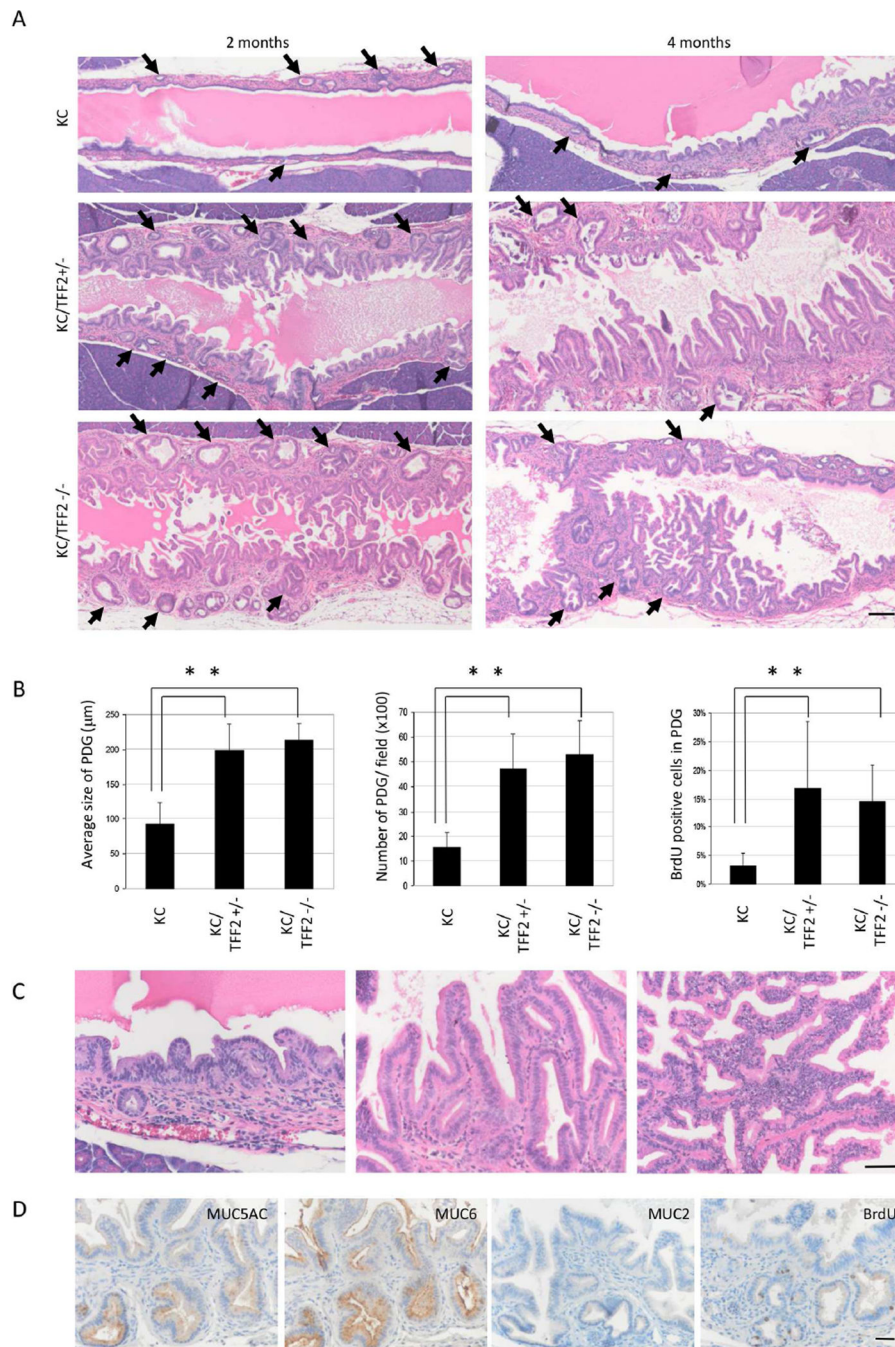


**Figure 4.**

Loss of TFF2 accelerates tumorization of KC mice. (A) While KC mice develop pseudopapillary lesions in the main pancreatic duct by 4 months, KC/TFF2KO mice show large papillary structures with increased PDG in both size and number (arrow) by 2 months. Scale Bars: 100 µm (B) Size, number and BrdU-positive PDG increase in both KC/TFF2<sup>+/-</sup> and KC/TFF2<sup>-/-</sup> mice ( $p < 0.05$ ). (C) Pseudo-papillary lesions in KC mice (left), low-grade papillary structure in KC/TFF2<sup>+/-</sup> mice (middle), high-grade papillary structure in KC/TFF2<sup>-/-</sup> mice (right). Scale Bars: 50 µm (D) Papillary structure in KC/TFF2<sup>-/-</sup> mice

express gastric mucins MUC5AC and MUC6. BrdU is incorporated in PDG compartment.  
Scale Bars: 50  $\mu$ m.

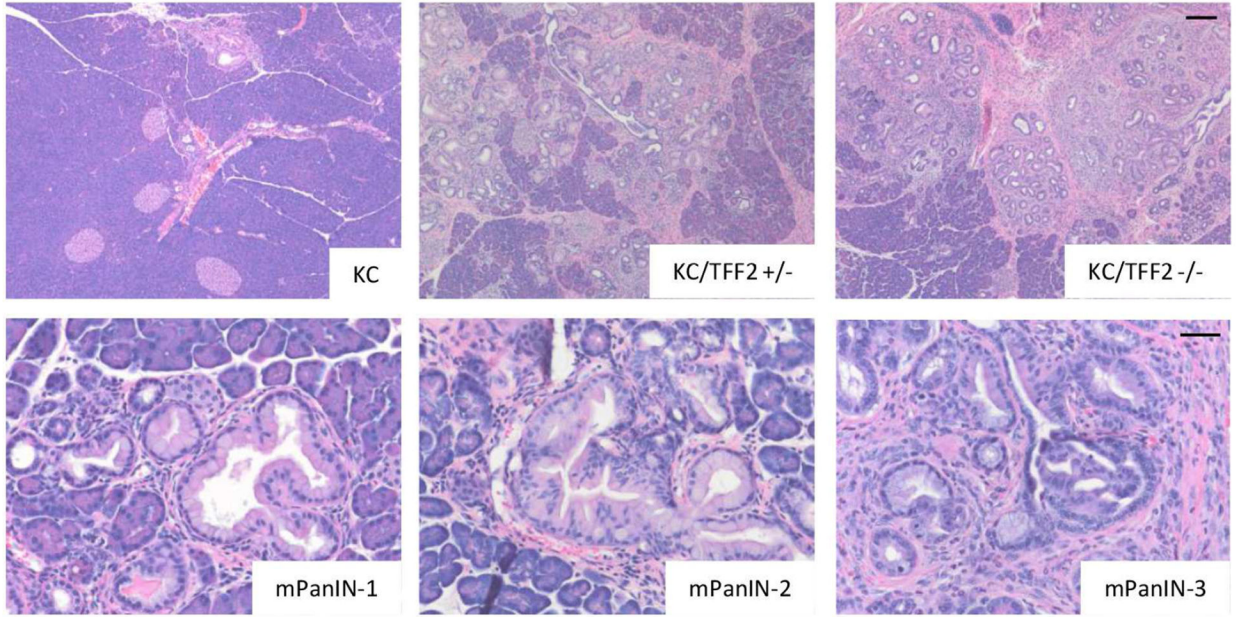
Author Manuscript

Author Manuscript

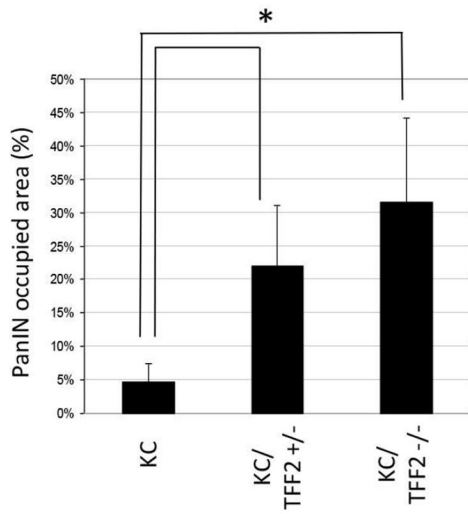
Author Manuscript

Author Manuscript

A



B



C

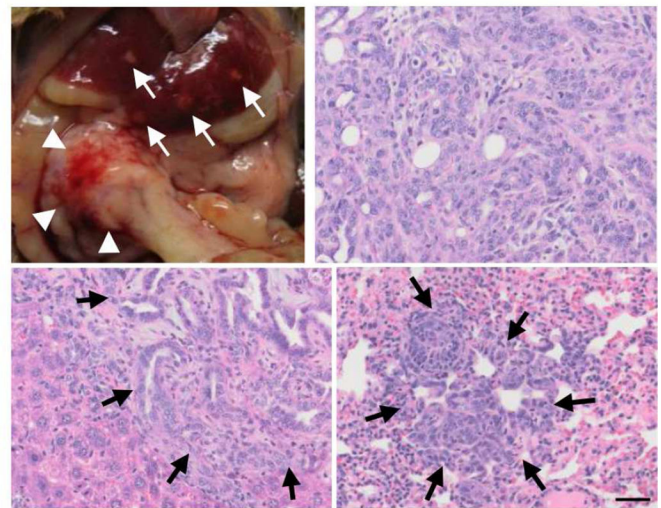


**Figure 5.**

Carcinogenesis in KC/TFF2KO mice at the age of 6 months. (A) While KC mice show only mPanIN-1 (left), KC/TFF2KO mice show mPanIN-2 (middle) and mPanIN-3 (right). Scale Bars: 200  $\mu$ m (top) and 50  $\mu$ m (bottom) (B) The PanIN-occupied area is significantly larger in TFF2-deficient mice ( $p < 0.01$ ). (C) A KC/TFF2 $^{+/-}$  mice was found to have PDAC in the pancreatic head (top, arrowheads) with multiple liver (top, white arrows: bottom, left, black arrows) and lung metastases (bottom, right, black arrows). Scale Bars: 50  $\mu$ m.

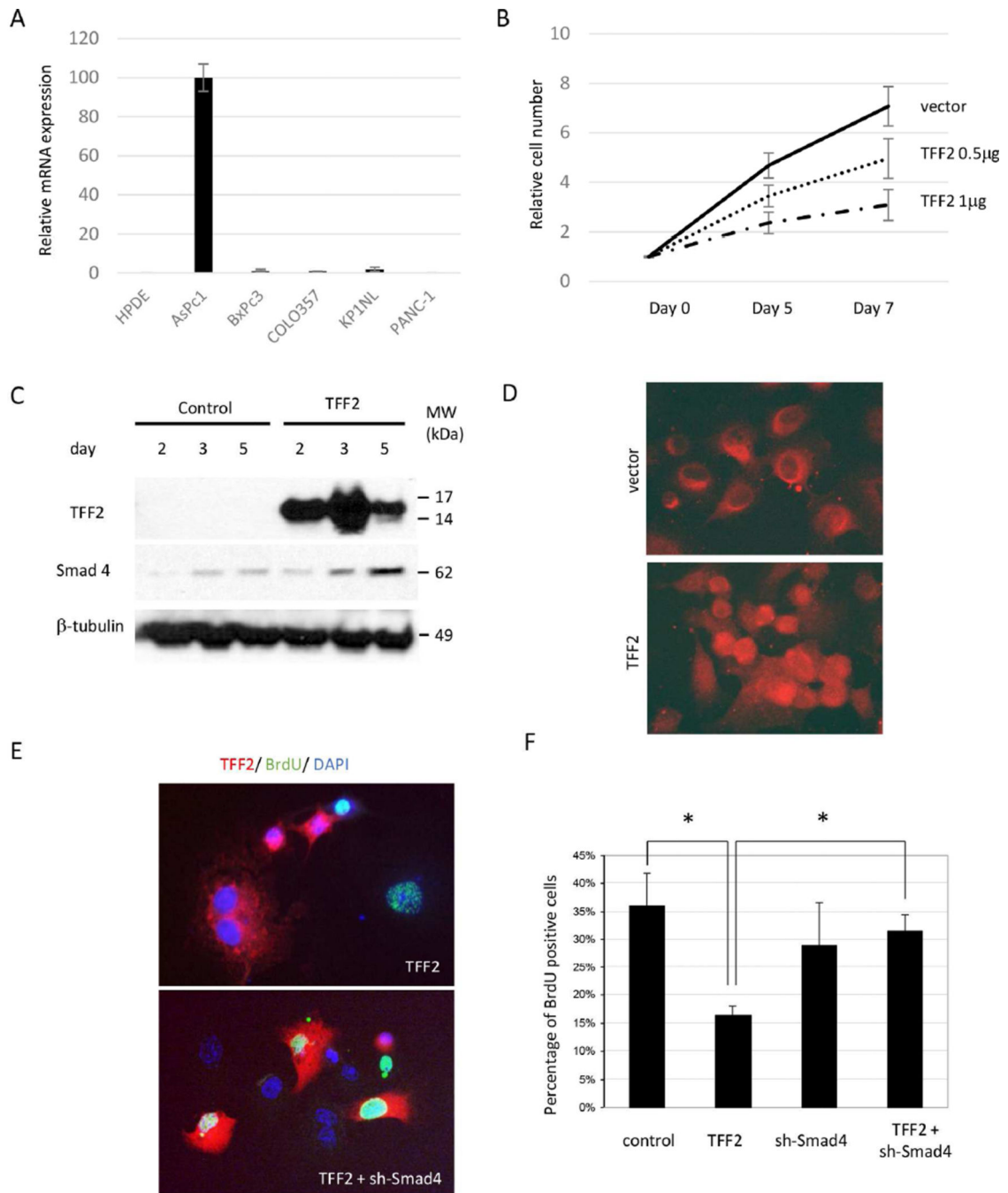


**Figure 6.** TFF2 inhibits cell-proliferation via SMAD4 *in vitro*. (A) RNA expression of TFF2 in HPDE and cancer cell lines (Real-Time PCR). (B) Growth curve showing TFF2 dose-dependent inhibitory effects on proliferation. (C) Overexpression of TFF2 induced upregulation of SMAD4. (D) SMAD4 expression can be found in nuclei after the overexpression of TFF2. (E) Double-positive cells for TFF2 and BrdU can be found after the suppression of SMAD4. (F) The downregulation of proliferation by TFF2 can be restored by the SMAD4.

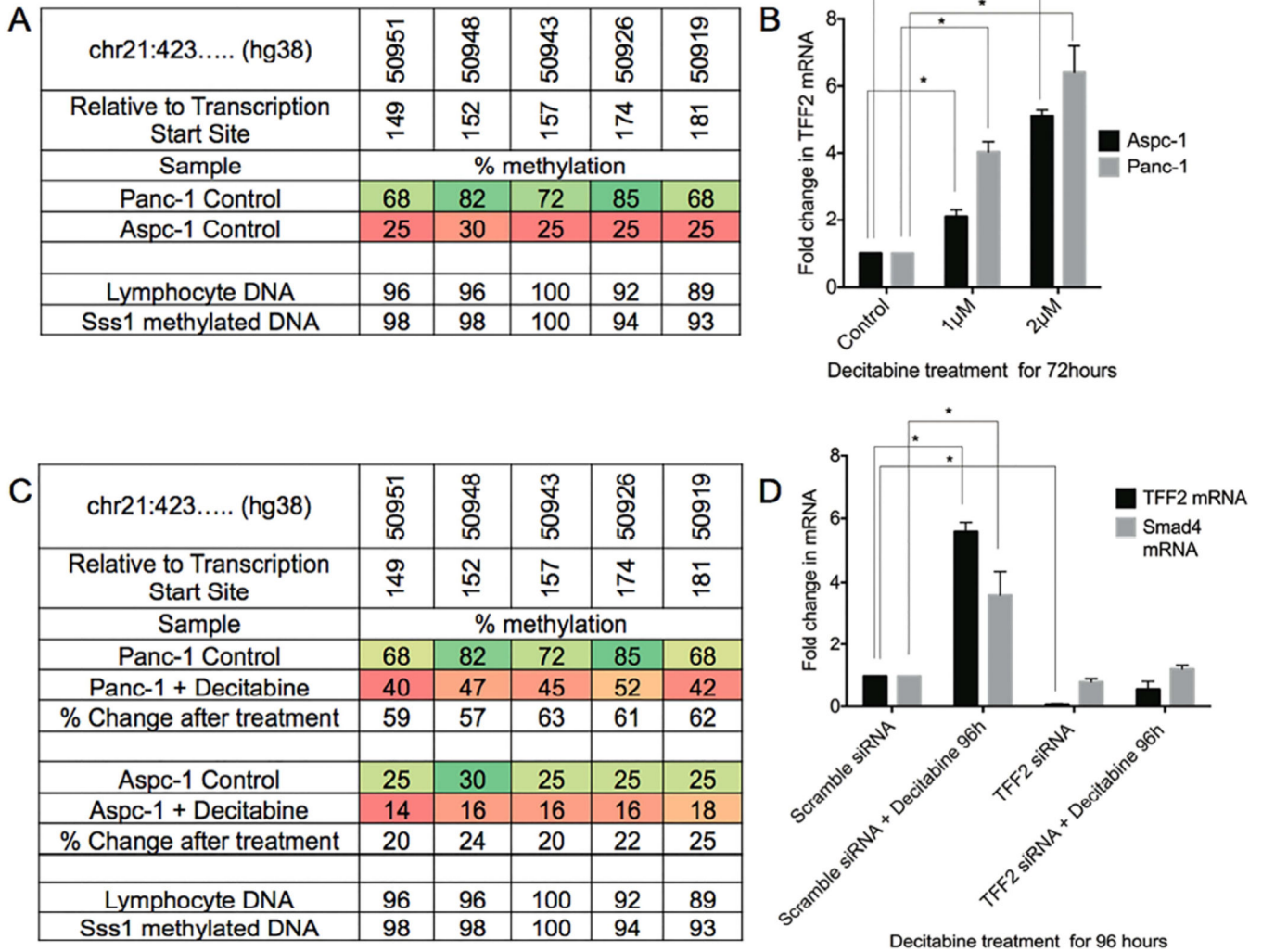


**Figure 7.** TFF2 promoter methylation and SMAD4 regulation *in vitro*. (A) TFF2 promoter DNA methylation profiles of PANC-1 and Aspc-1 cells. Lymphocyte DNA and Sss1 methylated DNA are used as controls. (B) TFF2 gene is upregulated following the genomic demethylation by decitabine. (C) After treatment with decitabine, promoter methylation in all the 5 CpG sites was decreased. (D) Treatment with decitabine upregulated TFF2 and SMAD4 mRNA. However, siRNA-mediated knockdown of TFF2 abrogated the decitabine-mediated SMAD4 upregulation.